ARTICLES

Probing Vibrational Dynamics of Hydrogen-Bonded Inclusion Compounds with Inelastic Neutron Scattering and Ab Initio Calculations

A. M. Pivovar,[†] M. D. Ward,*[,†] C. M. Brown,[‡] and D. A. Neumann*[,‡]

Department of Chemical Engineering and Materials Science, University of Minnesota, Amundson Hall, 421 Washington Avenue, S.E., Minneapolis, Minnesota 55455-0132, and the Center for Neutron Research, National Institute of Standards and Technology, Gaithersburg, Maryland 20899

Received: November 9, 2001; In Final Form: January 21, 2002

Guanidinium organodisulfonates form lamellar host lattices in which adjacent two-dimensional hydrogen-bonded sheets consisting of topologically complementary guanidinium cations (**G**) and sulfonate moieties (**S**) are connected by the organodisulfonates, which serve as pillars that support inclusion cavities, between the sheets, which are occupied by guest molecules. Inelastic neutron scattering (INS) at low energies (35−120 meV or 280−970 cm^{-1}) has been performed to probe the lattice dynamics of selected **GS** inclusion compounds. The pillars and the guests can be easily interchanged to produce inclusion compounds with various host−guest compositions, which can have different solid-state architectures but with retention of lamellar character. The specific host−guest combinations were chosen to evaluate the influence of the host environment on the vibrational modes of the guests, with particular attention paid to the role of pillar−guest isomorphism and lattice architecture. The multicomponent character of these materials enables selective isotopic labeling (hydrogen or deuterium) of the components—guanidinium ion, organodisulfonate pillar, and guest molecule—so that specific features in the INS spectra of the inclusion compounds can be assigned unambiguously to each component. These assignments are corroborated by ab initio density functional theory calculations for free, isolated guest molecules, which also define the specific molecular motions associated with each feature in the INS data. The INS spectra produced by the ab initio calculations are in excellent agreement with the experimental data, illustrating the accuracy of the assignments while also demonstrating the reliability of the calculations for predicting INS spectra and lattice dynamics. Overall, the contributions to the INS spectra from the guest molecules do not differ appreciably from those observed for crystals of the pure guests or predicted by ab initio calculations. This demonstrates that the host lattices examined here do not appreciably influence the dynamic behavior of the guest molecules, most likely reflecting the absence of strong host−guest interactions, specifically between the organodisulfonate pillars and the guests.

Introduction

One of our laboratories has recently reported a series of crystalline guanidinium−organosulfonates with solid-state architectures based on two-dimensional quasihexagonal hydrogen-bonded sheets consisting of topologically complementary guanidinium ions (**G**) and sulfonate (**S**) (Figure 1a).[1] This quasihexagonal motif, having been observed for numerous organomonosulfonates and organodisulfonates, is unusually persistent and has led to the design and synthesis of a rich variety of inclusion compounds for both mono- and disulfonates. To date, these inclusion compounds most commonly adopt lamellar architectures,[2] with the organodisulfonates serving as "pillars" that support inclusion cavities between the **GS** sheets. Unlike most other organic hosts, the size and shape of the inclusion cavities of the **GS** hosts can be systematically modified through judicious choice of the molecular pillar. This unique feature has enabled the synthesis of numerous isomorphous inclusion hosts, based on different organodisulfonate pillars, capable of including a variety of guest molecules with different sizes and shapes. Furthermore, different host−guest combinations can yield different host architectures, the two most common denoted as discrete bilayer and a continuous "brick," which differ with respect to the topological arrangement of the pillars from each **GS** sheet (Figure 1b).[3−5]

The persistence of the **GS** lamellar architectures for various organodisulfonate pillars and the ability of these hosts to include diverse guests make them ideal candidates for exploring fundamental structure−property relationships influenced by intermolecular packing. Measurements of guest affinity[6] and single-crystal X-ray diffraction provide substantial insight in this regard. These methods, however, are limited with respect to elucidating the vibrational *dynamics* and corresponding molecular motions of the host and guest components, which can affect guest retention in the host framework, chemical reactions between guest molecules inside the host, and charge

* Authors to whom correspondence should be addressed.
[†] University of Minnesota.
[‡] National Institute of Standards and Technology.

10.1021/jp014113w CCC: $22.00
Published on Web 04/24/2002

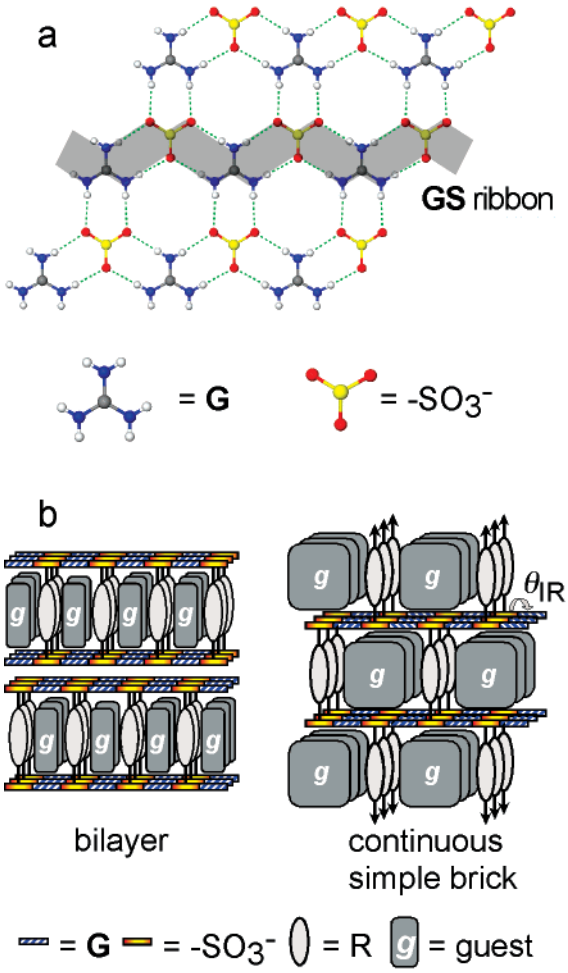

Figure 1. (a) Model of the quasihexagonal hydrogen-bonded guanidinium−sulfonate (**GS**) sheet. A single **GS** ribbon is highlighted in gray. The sheet can pucker about a flexible "hinge" defined by the hydrogen bonds that fuse these ribbons. (b) Schematic representation of **GS** inclusion compounds with the pillared discrete bilayer (left) and continuous simple brick host (right) architectures. The **GS** sheets in the brick architecture can pucker about the hydrogen bonds that fuse the ribbons, the puckering angle defined as q_{IR}.

transport among the components of the inclusion compound. Our interest in these topics, coupled with the availability of a wide variety of host−guest combinations for the **GS** compounds, prompted us to explore the low-energy dynamics of selected **GS** inclusion compounds with inelastic neutron scattering (INS) and theoretical ab initio calculations.

Though optical spectroscopic techniques (e.g., infrared and Raman) can be used to elucidate vibrational behavior,[7] they rely on symmetry-based selection rules and the nature of the response is seldom entirely a function of molecular motions. For example, the intensity of infrared or Raman spectral peaks can reflect a convolution of the atomic motions with the dipole moment and electronic polarizability of the molecules being probed. The theoretical description required for predicting the electronic response is rather complex, in some cases prohibiting comparisons of calculated and experimental spectra. These limitations make INS an attractive option for examining low-frequency vibrational modes in molecular materials. Neutrons have wavelengths comparable with interatomic distances and energies comparable to those associated with typical harmonic molecular motions, making them well suited for probing dynamic phenomena in solids. As neutrons interact primarily with atomic nuclei rather than electrons, the nature of the interaction is relatively simple to model, allowing straightforward comparison of experimental and theoretical data. Additionally, the large incoherent scattering cross section of hydrogen relative to all other nuclei produces spectra selective to vibrational modes involving hydrogen nuclei, thereby facilitating assignment of INS features to specific components.

The value of combined inelastic neutron scattering (INS) experiments and theoretical calculations for investigating the dynamics of organic materials has been amply demonstrated for a diverse variety of homomolecular crystals.[8] These investigations have demonstrated ab initio density functional theory (DFT) calculations to be the most suitable method for reliably reproducing experimental spectra. Due to the computational costs associated with DFT methods performed on systems with large numbers of atoms, however, this method has been somewhat limited in its application to inclusion compounds. Experimental INS studies of inclusion compounds based on urea[9−11] and calixarene hosts[12,13] have been performed and compared with spectra calculated using molecular dynamics and molecular mechanics calculations, respectively. Theoretical ab initio calculations have been used to calculate the vibrational spectrum of large catenane[14,15] molecular systems.

The specific **GS** host−guest combinations described herein—based on 4,4′-biphenyldisulfonate (**BPDS**) and 2,6-naphthalenedisulfonate (**NDS**) pillars—were chosen to evaluate the influence of the host environment on the vibrational modes of the guests, with particular attention paid to the role of pillar−guest isomorphism and lattice architecture. The multicomponent character of these materials enables selective isotopic labeling (hydrogen or deuterium) of the components—guanidinium ion, organodisulfonate pillar and guest molecule—so that specific features in the INS spectra of the inclusion compounds can be assigned unambiguously to each component. The experimental INS spectra are in excellent agreement with those produced by ab initio calculations, corroborating the assignments while also demonstrating the reliability of the calculations for predicting INS spectra and vibrational dynamics in organic crystals. The combined experimental data and calculations suggest that host composition and architecture do not appreciably influence the dynamic behavior of the guest molecules, most likely reflecting the absence of strong host−guest interactions, specifically those between the organodisulfonate pillars and the guests.

Experimental Section

Materials and General Procedures. Single crystals of the guanidinium biphenyldisulfonate clathrates, $(\mathbf{G})_2(\mathbf{BPDS})\cdot n$(guest), were grown at room temperature by combining equal volumes of saturated methanol solutions containing the appropriate host and guest components, then allowing the combined solution to evaporate slowly. Single crystals containing various combinations of hydrogenated and deuterated components—guanidinium ion, organodisulfonate pillar, and guest molecule—were prepared with isotopically substituted components. The 4,4′-biphenyldisulfonate and 4,4′-biphenyldisulfonate-d_8 pillar components were prepared by a slightly modified version of a previously published procedure.[16] All starting materials, guest molecules, and solvents were purchased from Aldrich as ACS grade and were used as received. The host components were obtained as acetone clathrates by reaction of guanidinium tetrafluoroborate, prepared by neutralization of guanidinium carbonate with tetrafluoroboric acid, and the corresponding organodisulfonic acid in acetone. These compounds readily lose their enclathrated acetone under ambient conditions to yield pure, guest-free apohosts. The crystallization

of (**G**-d_6)$_2$(**BPDS**)·3(biphenyl-d_{10}) and (**G**-d_6)$_2$(**BPDS**-d_8)·3(biphenyl) was performed in CH_3OD in order to avoid deuteron/proton exchange between **G**-d_6 and CH_3OH.

Host Components. *[Guanidinium]$_2$[4,4′-biphenyldisulfonate], (**G**)$_2$(**BPDS**).* Biphenyl (9.86 g, 63.9 mmol) was added to 100 mL concentrated sulfuric acid at 150 °C with stirring. Upon addition of the biphenyl the reaction mixture achieved a slight pink color. After 1 h, heating was stopped and the reactants were allowed to cool to room temperature. The cooled reaction mixture was quenched by the addition of ca. 50 mL of ice, and 100 mL of a saturated potassium chloride aqueous solution was added. After approximately 10 min, numerous small, white crystals of K_2(**BPDS**) formed in the flask. These crystals were retrieved by filtration and recrystallized from water three times. The recrystallized K_2(**BPDS**) was dissolved in water and converted to the barium salt Ba(**BPDS**) by addition of a saturated $BaCl_2$ solution. The resulting Ba(**BPDS**) precipitate was retrieved by filtration and dried in a vacuum oven for ∼12 h. The dried Ba(**BPDS**) (18.6 g) was dispersed in water and converted to 4,4′-disulfonic acid by adding 1.1 molar equivalents of concentrated H_2SO_4 (5.00 g). The $BaSO_4$ byproduct was isolated by filtration and the filtrate containing the 4,4′- **BPDS** acid was dried in vacuo, resulting in a semicrystalline slurry. This slurry was dissolved in 50 mL of acetone and treated with an acetone solution containing an excess of **G**[BF_4], affording (**G**)$_2$(**BPDS**)·acetone as a white precipitate, which was retrieved by filtration and dried to give the pure apohost material (11.6 g, 30.2 mmol, 47.2% yield).

*[Guanidinium-d_6]$_2$[4,4′-biphenyldisulfonate], (**G**-d_6)$_2$(**BPDS**).* Isotopic substitution of the guanidinium hydrogen atoms of (**G**)$_2$(**BPDS**) with deuterium was achieved by proton exchange with D_2O. This was achieved by dissolving approximately 5 g of (**G**)$_2$(**BPDS**) in 25 g of D_2O followed by evaporation of the solution to dryness in vacuo. The molar ratio of deuterium to exchangeable guanidinium protons is approximately 16 to 1 under these conditions. The D_2O exchange was repeated 7 times to ensure maximal exchange of hydrogen with deuterium and confirmed by the absence of guanidinium amine peaks in ^{1}H NMR spectroscopy.

*[Guanidinium]$_2$[4,4′-biphenyldisulfonate-d_8], (**G**)$_2$(**BPDS**-d_8).* Addition of 10.42 g (63.4 mmol) of biphenyl-d_{10} to 100 mL of D_2SO_4 at 150 °C with stirring resulted in the immediate formation of a black reaction mixture. This discoloration, which does not appear under identical conditions with undeuterated biphenyl, is believed to result from impurities in the biphenyl-d_{10} starting material. After stirring for 1 h, the dark reaction mixture was allowed to cool to room temperature. The cooled black mixture was quenched by the addition of ca. 50 mL of deuterated ice. The addition of 100 mL of a D_2O solution saturated with KCl afforded numerous small dark brown crystals of K_2(**BPDS**-d_8). The colored crystals were retrieved by filtration and dissolved in 100 mL of D_2O to afford a dark brown solution, which was stirred over activated carbon and filtered repeatedly until the resulting filtrate was nearly colorless. The purified K_2(**BPDS**-d_8) was retrieved by evaporation of colorless filtrate, recrystallized from D_2O three times, and converted to Ba(**BPDS**-d_8) by the addition of D_2O saturated with $BaCl_2$. After filtration and drying, the Ba(**BPDS**-d_8) (15.85 g) was converted to the acid with 1.1 molar equivalents of concentrated D_2SO_4 (3.9 g) in D_2O. The $BaSO_4$ precipitate was removed by filtration and the filtrate containing the organodisulfonic acid was evaporated under vacuum and the oily appearing residue dissolved in acetone. The solution was treated with an acetone solution of **G**[BF_4] to precipitate (**G**)$_2$(**BPDS**-d_8)·acetone as a white powder, which was filtered and dried in vacuo to yield 9.84 g (22.3 mmol) of the apohost (35.3% overall yield).

*[Guanidinium-d_6]$_2$[4,4′-biphenyldisulfonate-d_8], (**G**-d_6)$_2$(**BPDS**-d_8).* Isotopic exchange of the guanidinium hydrogen atoms for deuterium was performed on (**G**)$_2$(**BPDS**-d_8) using the procedure described above for (**G**-d_6)$_2$(**BPDS**).

*[Guanidinium]$_2$[2,6-naphthalenedisulfonate], **G**$_2$(**NDS**).* The disodium salt of 2,6-naphthalenedisulfonate (approximately 10 g) was converted to its acidic form by aqueous ion-exchange using Amberlyst[17] 36(wet) ion-exchange resin (Aldrich). The exchanged solution was evaporated to dryness in vacuo to yield 2,6-naphthalenedisulfonic acid as a white powder. The acid was then dissolved in acetone and mixed with an acetone solution containing an excess of **G**[BF_4], resulting in the immediate formation of **G**$_2$(**NDS**) as a white precipitate, which was retrieved by filtration.

Neutron Scattering. INS data was collected with the filter analyzer spectrometer (FANS) located on beam tube BT-4 at the National Institute of Standards and Technology Center for Neutron Research, Gaithersburg.[18] This instrument produces monochromatic neutrons with initial energy E_i selected from a polychromatic beam of neutrons emanating from the reactor core by Bragg diffraction from a copper Cu(220) monochromator. The neutron beam is focused on the sample by collimators with 40 minutes of arc divergence, scattered inelastically through ∼90°, and then passed through Bragg cutoff filters of polycrystalline beryllium and powdered graphite before detection. The cutoff filters remove all neutrons with energy greater than ∼1.8 meV and, as a result of the specific geometry of the instrument, yields an energy resolution of ∼1.1 meV. The FANS instrument is able to scan energy ranges between 25 and 220 meV (i.e., from 200 to 1760 cm^{-1}), though this investigation uses only the 35−120 meV range.

Prior to collecting INS spectra, the inclusion compounds crystals were thoroughly rinsed with acetone to remove any pure guest material that may have crystallized simultaneously with the clathrate compounds. The samples were then dried and loaded into flat aluminum sample holders (approximately 4 g). The sample holders containing the inclusion compounds were attached to the coldfinger of a He displex and the INS spectra recorded at ∼10 K. All experimentally obtained spectra presented herein have been scaled to a per mass basis and background adjusted by subtracting the spectrum obtained on an empty sample holder under identical conditions.

Ab Initio Calculations. Ab initio calculations to determine the harmonic vibrational modes of the guest molecules were performed in order to facilitate interpretation of the experimental INS spectra. The calculations were executed on single, isolated biphenyl, anthracene, and naphthalene molecules using the *Gaussian 98* program[19] module contained in the Cerius^2 software package employing the B3LYP density functional approximation and 6-31-G* basis set. The vibrational behavior generated by the calculation is summarized in a dynamical matrix containing the eigenvectors (atomic displacement trajectories) and eigenvalues (frequency of displacement), which correspond to the observed vibrational intensity and energy, respectively. This calculated vibrational behavior can be converted into a "theoretical" INS spectrum by broadening the vibrational intensity in accordance with the resolution of the FANS instrument measured at 40 minutes of arc divergence and an appropriate Debye−Waller factor (ca. 0.1). The absolute intensity of the theoretical spectrum is then uniformly scaled to permit facile comparison with the relative peak intensities of the experimental data.

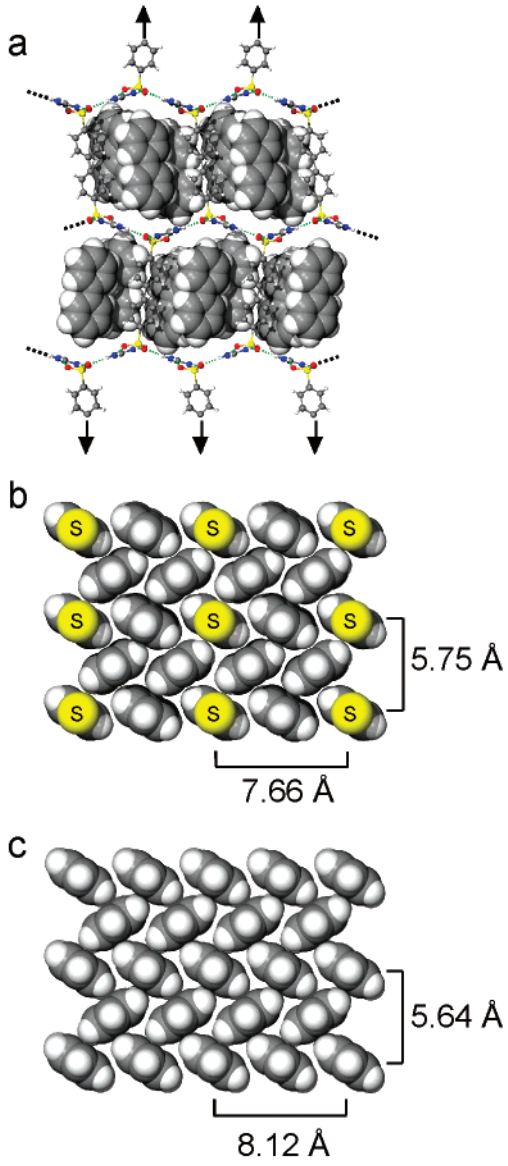

Figure 2. (a) The crystal structure of $\mathbf{G}_2$(**BPDS**)·3(biphenyl), as viewed parallel to the **GS** sheets, revealing the brick-like architecture and puckering of the **GS** sheets. The guests are rendered as space filling. (b) Top view of the herringbone packing of the pillars and guests between the **GS** sheets. The guanidinium ions and the sulfonate oxygen atoms of the upper GS sheet have been removed so the packing can be viewed. The pillars can be identified by the sulfur atoms. (c) Top view of the herringbone packing in pure biphenyl.

Results and Discussion

Previous single-crystal X-ray diffraction studies[2a] revealed that $\mathbf{G}_2$(**BPDS**)·3(biphenyl) exhibits the simple brick architecture in which the pillar and the isostructural guests pack in a two-dimensional motif that mimics the herringbone packing observed in crystals of pure biphenyl[20] (Figure 2). Herringbone packing in $\mathbf{G}_2$(**BPDS**)·3(biphenyl) is achieved because (i) puckering of the **GS** sheets results in contraction of the lattice along a direction perpendicular to the **GS** ribbons, thereby allowing dense packing of the pillars and guests, and (ii) free rotation of the organodisulfonate pillars about their C−S bonds permits the pillars to rotate into positions conducive to the herringbone motif. This compound provides a unique opportunity for probing the influence exerted by the host lattice on the guest dynamics, as each guest is confined within an environment that effectively

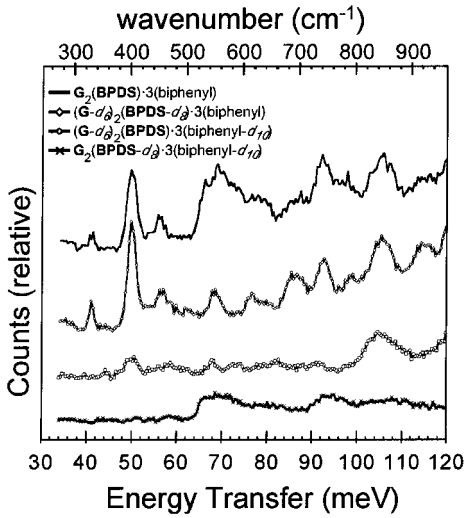

Figure 3. INS spectra collected on single crystals of $\mathbf{G}_2$(**BPDS**)·3(biphenyl) and single crystals comprising the three possible permutations of isotopically substituted components, wherein two of the three compoqnents—**G** ions, organodisulfonate pillars, and guests—are deuterated so that only the remaining one contributes to neutron scattering.

mimics its native structure but with the added constraint of the isostuctural pillar being anchored to the **GS** sheets of the host.

The overall (i.e., all components fully hydrogenated) INS spectrum of $\mathbf{G}_2$(**BPDS**)·3(biphenyl) is depicted in Figure 3. This figure also illustrates data collected on crystals comprising the three possible permutations of isotopically substituted components, wherein two of the three components—**G** ions, organodisulfonate pillars, and guests—are deuterated so that only the remaining one dominates the neutron scattering. These spectra, therefore, systematically reveal the individual contributions of each component to the dynamic behavior of the overall structure. Each spectrum has been background corrected and scaled on a per mass basis in order to simplify comparison. Over the 35−120 meV energy range (1 meV = 8.07 cm^{-1}), the overall spectrum exhibits several distinct features that, by inspection, can be directly attributed to specific components of the inclusion compound. Most obvious are the three peaks observed at 41, 50, and 56 meV, which are exclusively associated with the corresponding peaks observed in the (**G**-d_6)$_2$(**BPDS**-d_8)·3(biphenyl) spectrum and, therefore, can be ascribed to molecular motions of the guest molecules. The broad band of the overall spectrum in the 64−81 meV range results from the overlap of two distinct peaks at 68 and 77 meV of the guest and a broad peak in the spectrum selective to the guanidinium ions covering the 64−74 meV energy range. The poorly resolved feature in the spectrum of the fully hydrogenated material from 84 to 89 meV can be attributed to guest motions. The peak at 92 meV, with its shoulder that tails to 100 meV, reflects overlapping contributions from the guest (a medium intensity peak at 92 meV and a weak peak at 98 meV) and guanidinium ions (a broad peak ranging from 91 to 98 meV). The broad peak in the overall spectrum centered at ∼105 meV results from overlapping contributions due to motions of both the guests and the pillars.

Inspection of Figure 3 reveals that most of the distinct features in the INS data collected for $\mathbf{G}_2$(**BPDS**)·3(biphenyl) can be attributed to the guests alone. This perhaps is not surprising, as the number of hydrogen atoms on the guest molecules (60% of the total complex) is large relative to the host components. Over the investigated energy range, several low energy modes corresponding to the internal vibrations of the biphenyl guests

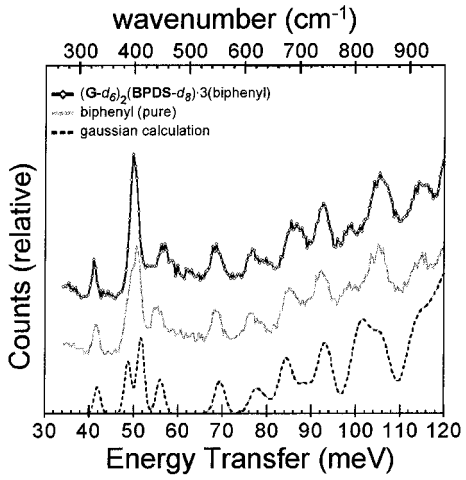

Figure 4. Experimental INS spectra of (**G**-d_6)$_2$(**BPDS**-d_8)·3(biphenyl) (top), pure biphenyl (middle) and a spectrum constructed from the results of an ab initio calculation performed on a single, isolated biphenyl molecule (bottom).

are observed. For the spectrum selective to motions of the pillars, however, only one peak is observed. This suggests that most pillar vibrations occur at energies greater than 120 meV, which can be rationalized by considering the constraint placed on its molecular motion by the hydrogen-bonded sheets. The energy of vibrational bands observed for **G**$_2$(**BPDS**-d_8)·3(biphenyl-d_{10}) compare favorably with those observed by INS for guanidinium in crystalline guanidinium nitrate[21] and guanidinium methanesulfonate,[22] wherein the broad bands at 64−74 meV and 91−98 meV were assigned to multiple wagging and twisting vibrational modes of the amine groups.

To ascertain the influence of the host lattice on the dynamic behavior of the guest molecules, an INS spectrum on pure biphenyl was collected and compared with that obtained for (**G**-d_6)$_2$(**BPDS**-d_8)·3(biphenyl) (Figure 4). Other than a slight shift in the single peak at 56 meV, it is apparent that both the intensity and frequency of all peaks in the pure biphenyl spectrum replicate those obtained for biphenyl included within the host lattice. It is evident, therefore, that the host framework in this isostructural pillar/guest system exerts no appreciable influence, relative to pure biphenyl crystals, on the dynamic behavior of the biphenyl guest molecules.

Attempts to make vibrational mode assignments of the observed INS peaks collected from (**G**-d_6)$_2$(**BPDS**-d_8)·3(biphenyl) complex using the INS data and previously reported theoretical calculations for pure biphenyl were not entirely satisfactory, largely because the previous reports were either too qualitative in nature or spanned an energy range that was too large to permit adequate resolution of peaks for accurate comparison with this study.[23,24] It was necessary, therefore, to perform our own ab initio calculations on biphenyl in order to assign specific molecular motions to the INS peaks for the guests in the **GS** inclusion compounds. This was accomplished by executing geometry optimization and normal mode calculations using the *Gaussian 98* program on a single, isolated biphenyl molecule. The results of this vibrational analysis were broadened to reflect the resolution of the FANS instrument and the entire spectrum scaled uniformly to best fit the experimental data (Figure 4). Examination of the calculated, pure biphenyl and biphenyl-as-guest spectra reveals extremely good agreement over the 35−120 meV energy range, thereby corroborating the assignments made by isotopic labeling and also establishing the reliability of the ab initio calculations for assignment of the observed vibrational modes contributed by the guest molecules. The only

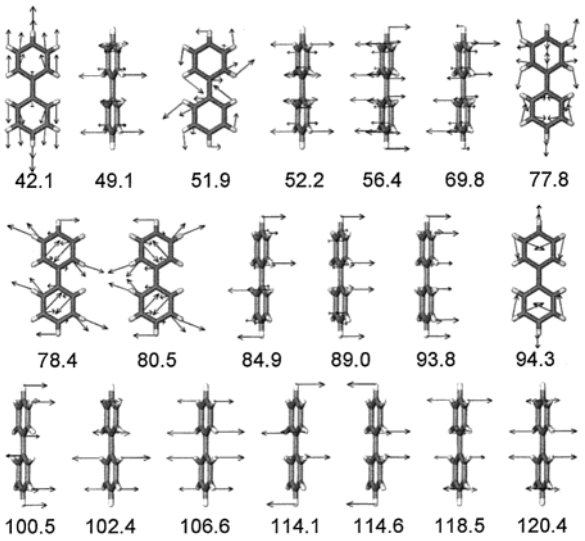

Figure 5. Schematic representation of the atomic trajectories of each normal vibrational mode of biphenyl between 35 and 120 meV as determined by an ab initio calculation. The relative magnitudes of the arrows correspond to the atomic displacement in one-quarter of the overall vibration. Energies are provided in units of meV (1 meV = 8.07 cm^{-1}).

noticeable discrepancy between the calculated and experimental spectra arises in the two peaks of the calculated spectrum at 48 and 52 meV, which are not individually resolved in either experimental spectrum. Trajectories defining the atomic displacements of the biphenyl molecule for each of the calculated normal modes are schematically depicted in Figure 5. The mode observed at 56.4 meV in both pure biphenyl and the Gaussian calculation is shifted to slightly higher energy for biphenyl guests in the **G**$_2$(**BPDS**) host, possibly reflecting a weak steric constraint of the guest molecule motion by the anchored **BPDS** pillars.

The structure of **G**$_2$(**BPDS**)·3(anthracene) resembles that of **G**$_2$(**BPDS**)·3(biphenyl), having both a simple brick architecture and herringbone-like packing of the biphenyl pillar and anthracene guest molecules (Figure 6). This herringbone-like packing of the pillars and guest is similar to that observed in pure anthracene crystals,[25] but with one out of every four anthracene molecules replaced by a **BPDS** pillar. In this compound, the pillar and guest are not isostructural, providing a means to probe the influence of pillar structure on the dynamic behavior of guest molecules.

The INS spectrum of completely hydrogenated **G**$_2$(**BPDS**)·3(anthracene) in Figure 7 reveals three distinct spectral features at the low-end of the spectrum—as a shoulder at ca. 35 meV and two well-defined single peaks at 49 and 61 meV. A rather broad, but pronounced peak occurs over 65 to 76 meV with a shoulder tapering off around 86 meV. Another broad peak is observed over the 89−100 meV energy range, followed by a convoluted band from 100 to 115 meV. The higher energy portion of the spectrum shows a sharp increase in intensity up to the scan limit of 120 meV.

The contribution of the anthracene guest molecules to the INS spectra of **G**$_2$(**BPDS**)·3(anthracene) was assigned by calculating the spectrum of a single anthracene molecule using *Gaussian 98* (Figure 7). The accuracy of the calculated spectrum was confirmed by comparison with the reported INS spectrum of anthracene taken at 4.7 K by Bokhenkov et al.[26] Several calculated peaks precisely match those observed in the experimental INS spectrum of **G**$_2$(**BPDS**)·3(anthracene) (49, 61, 89−100, 102−112 meV and the low and high energy shoulders at

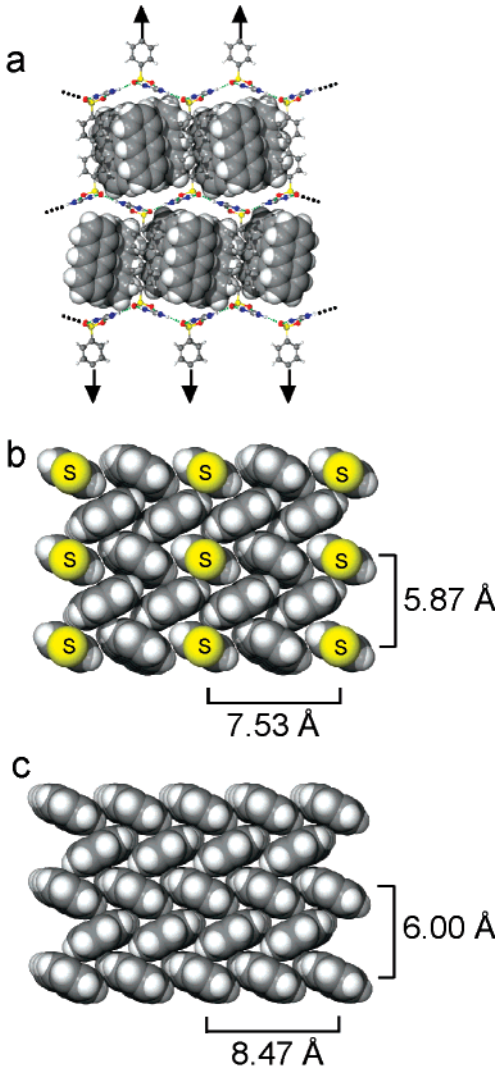

Figure 6. (a) The crystal structure of $\mathbf{G}_2$(**BPDS**)·3(anthracene) as viewed parallel to the **GS** sheets, revealing the brick-like architecture and the puckering of the **GS** sheets. The guests are rendered as space-filling. (b) Top view of the herringbone packing of the pillars and guests between the **GS** sheets. The guanidinium ions and the sulfonate oxygen atoms of the upper **GS** sheet have been removed so the packing can be viewed. The pillars can be identified by the sulfur atoms. (c) Top view of the herringbone packing in pure anthracene.

ca. 35 and 120 meV), permitting assignment of these peaks to molecular motions of the guest molecules. The calculation also reveals that a small portion of the broad spectral bands observed in the 65 to 86 meV range can be ascribed to the anthracene guests. The atomic trajectories and frequency of all anthracene normal modes, as determined by *Gaussian 98* within the 35−120 meV range, are depicted in Figure 8. The agreement between the experimental INS spectra of $\mathbf{G}_2$(**BPDS**)·3(anthracene) and the ab initio calculation for an isolated anthracene molecule indicates that the host lattice does not exert an appreciable influence on the dynamic behavior of the guest molecules.

The crystal structure of $\mathbf{G}_2$(**BPDS**)·3(anthracene) (a = 7.5265, b = 26.9704, c = 11.7435, a = g = 90, b = 91.076, q_{IR} = 128.2°) is nearly identical to that of $\mathbf{G}_2$(**BPDS**)·3(biphenyl) (lattice parameters: a = 7.7096, b = 26.3615, c = 11.5544, a = g = 90, b = 90.517, q_{IR} = 130.0°). It is reasonable to assume, therefore, that the dynamic behavior of the host frameworks is also similar. Combination of the calculated spectra for anthracene with contributions from the pillar and guanidinium ion,

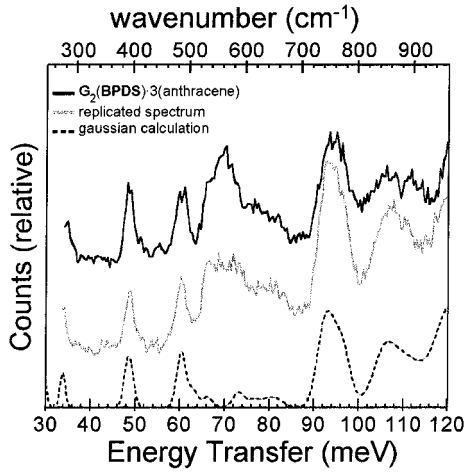

Figure 7. (top) An INS spectrum collected on $\mathbf{G}_2$(**BPDS**)·3(anthracene). (middle) A spectrum constructed by additive combination of $\mathbf{G}_2$(**BPDS**-d_8)·3(biphenyl-d_{10}), ($\mathbf{G}_2$-d_6)(**BPDS**)·3(biphenyl-d_{10}), and the spectrum calculated ab initio for an isolated anthracene molecule (bottom).

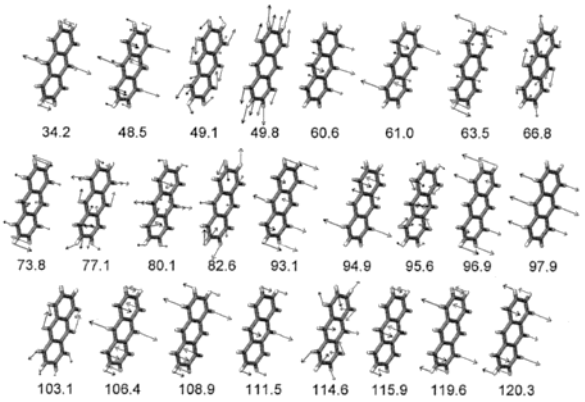

Figure 8. Schematic representation of the atomic trajectories of each normal vibrational mode of anthracene between 35 and 120 meV as determined by an ab initio calculation. The relative magnitudes of the arrows correspond to the atomic displacement in one-quarter of the overall vibration. Energies are provided in units of meV (1 meV = 8.07 cm^{-1}).

experimentally determined from ($\mathbf{G}$-d_6)$_2$(**BPDS**)·3(biphenyl-d_{10}) and $\mathbf{G}_2$(**BPDS**-d_8)·3(biphenyl-d_{10}), respectively, replicates the INS spectrum of completely hydrogenated $\mathbf{G}_2$(**BPDS**)·3(anthracene). Only a slight discrepancy in the relative intensity of the peaks above 90 meV is observed (Figure 7). This demonstrates the ability to determine a priori the INS spectra of materials based on guanidinium organodisulfonate hosts using ab initio calculations and data collected on homologous structures, thereby reducing the number of INS experiments necessary to assemble a catalog of the dynamic behavior expected from a large set of these materials.

To determine the influence of host architecture on guest vibrational modes, INS spectra were collected on a bilayer inclusion compound—$\mathbf{G}_2$(**BPDS**)·(naphthalene) —that allowed facile comparison with simple brick forms. Unlike the aforementioned simple brick compounds, including the homologous $\mathbf{G}_2$(**NDS**)·3(naphthalene), single-crystal diffraction of $\mathbf{G}_2$(**BPDS**)·(naphthalene) exhibits a "shifted-ribbon" hydrogen bonding motif wherein only five of the possible six hydrogen bonding interactions are fulfilled (Figure 9). Herringbone packing is observed in this bilayer structure,[27] but each naphthalene guest molecule is surrounded by four nearest neighbor pillars, compared with only two in a simple brick structure. It seemed reasonable to consider that the additional degree of guest

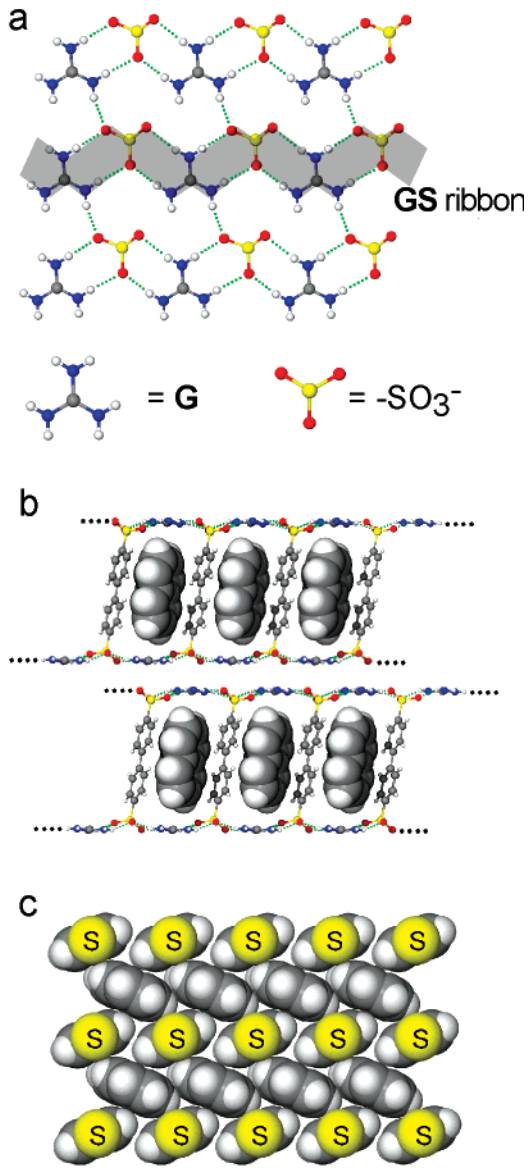

Figure 9. (a) The "shifted ribbon" hydrogen-bonded motif within a GS sheet. The gray shading highlights a single **GS** ribbon and, like the quasihexagonal motif, the sheet can pucker about a flexible "hinge" defined by the hydrogen bonds that connect these ribbons. (b) The crystal structure of the $\mathbf{G}_2$(**BPDS**)·naphthalene, as viewed parallel to the **GS** sheets, revealing the bilayer architecture. The guests are rendered as space-filling. (b) Top view of the herringbone packing of the pillars and guests between the **GS** sheets. The guanidinium ions and the sulfonate oxygen atoms of the upper **GS** sheet have been removed so the packing can be viewed. The pillars can be identified by the sulfur atoms.

confinement by host pillars would constrain guest motion to a further degree than observed in the simple brick hosts, where the constraint was negligible.

The INS spectra collected on bilayer $\mathbf{G}_2$(**BPDS**)·(naphthalene) crystals are depicted in Figure 10. Comparison of the $\mathbf{G}_2$(**BPDS**)·(naphthalene) and $\mathbf{G}_2$(**BPDS**)·(naphthalene-d_8) spectra allow assignment of specific features to naphthalene guest motion. The peaks at 45 and 58 meV (indicated by *), in the spectrum of the fully hydrogenated material can be exclusively attributed to guest motions. Since the relative intensity of the peak at 49 meV is reduced upon substitution with deuterated guest but is still evident, it contains contributions from both the host and guest components. No discernible peaks resulting from guest dynamics are observed at frequencies >60 meV.

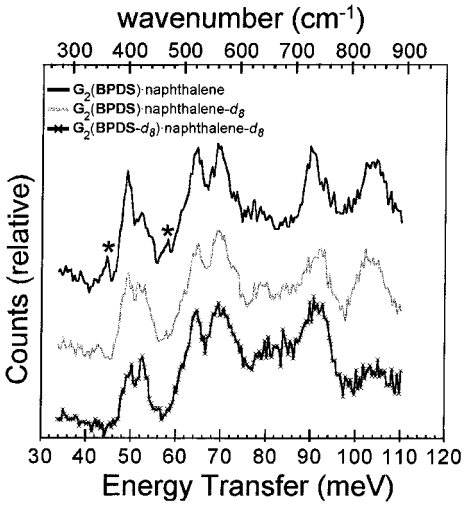

Figure 10. INS spectra collected on (top) single crystals of $\mathbf{G}_2$(**BPDS**)·(naphthalene), (middle) $\mathbf{G}_2$(**BPDS**)·(naphthalene-d_8), and (bottom) $\mathbf{G}_2$(**BPDS**-d_8)·(naphthalene-d_8).

Comparison of these spectra with data collected for $\mathbf{G}_2$(**BPDS**-d_8)·(naphthalene-d_8) indicates that the only significant contribution of the pillar in experimental energy range is the peak centered at ca. 105 meV. The remaining features, two sets of overlapping double peaks spanning 48−55 and 60−77 meV and a broad peak at 88−96 meV, can be attributed to the **G** ions. It should be noted that the bilayer structure has a guanidinium/pillar/guest ratio of 2:1:1, whereas in the brick structure this ratio is 2:1:3. Consequently, the relative intensity of peaks due to the host in the bilayer should be somewhat larger than that for simple brick hosts such as $\mathbf{G}_2$(**BPDS**)·3(biphenyl) (see Figure 3). Indeed, the $\mathbf{G}_2$(**BPDS**-d_8)·(naphthalene-d_8) data clearly reveal that the intensity contribution from the **G** ions to the spectrum of the fully hydrogenated material is much larger relative to that for this brick inclusion compound. The signal observed over 48−55 meV in the bilayer $\mathbf{G}_2$(**BPDS**-d_8)·(naphthalene-d_8), corresponding to modes involving the guanidinium ions and is shifted to significantly lower energy compared with the corresponding modes observed for $\mathbf{G}_2$(**BPDS**-d_8)·3(biphenyl-d_{10}). This shift is most likely associated with the shifted ribbon motif in this compound, in which only five protons of each **G** ion form strong hydrogen bonds to neighboring sulfonate moieties (four within the ribbon and one between adjacent ribbons), with the sixth (**G**)N−H···O(**S**) distance being larger to the extent that hydrogen bonding is weaker. This would anticipate a more shallow energy well for the harmonic motion of the guanidinium amine groups, thereby lowering the frequency of this vibrational mode.

Figure 11 provides a comparison of the INS spectrum collected for single crystals of bilayer $\mathbf{G}_2$(**BPDS**)·(naphthalene), brick $\mathbf{G}_2$(**NDS**)·3(naphthalene), and an ab initio calculation for a naphthalene molecule. The spectra principally differ at 48−52 and 90−110 meV, the former most likely reflected the different environments of the guanidinium ion in the "shifted ribbon" and quasihexagonal motifs of $\mathbf{G}_2$(**BPDS**)·(naphthalene) and the of $\mathbf{G}_2$(**NDS**)·3(naphthalene), respectively. Within the 90−110 meV range, $\mathbf{G}_2$(**NDS**)·3(naphthalene) exhibits a single, broad peak but $\mathbf{G}_2$(**BPDS**)·(naphthalene) exhibits two broad peaks at 92 and 105 meV. These differences are tentatively attributed to contributions from guanidinium ions and pillars in the different architectures.

The ab initio spectrum of naphthalene allow assignment of several peaks observed for $\mathbf{G}_2$(**BPDS**)·(naphthalene) and $\mathbf{G}_2$(**NDS**)·3(naphthalene). All of the calculated peaks for naph-

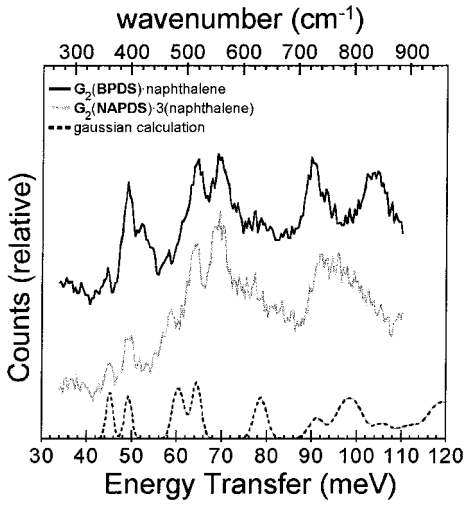

Figure 11. Experimental INS spectra of (top) bilayer $\mathbf{G}_2$(**BPDS**)·(naphthalene) and (middle) simple brick $\mathbf{G}_2$(**NDS**)·3(naphthalene), and (bottom) the spectrum constructed from the results of an ab initio calculation performed on a single, isolated naphthalene molecule (bottom).

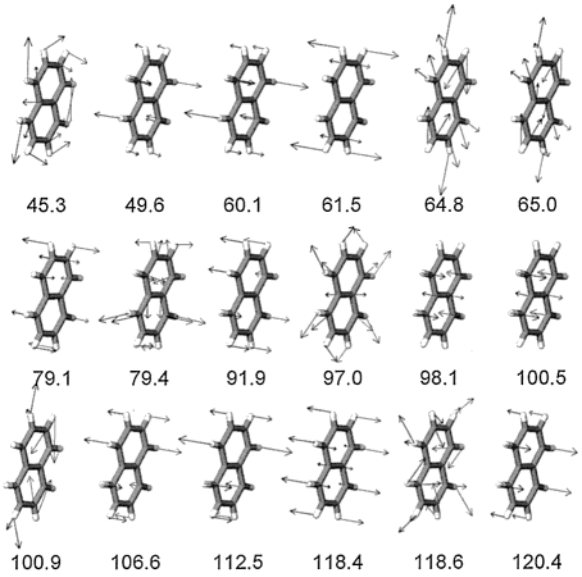

Figure 12. Schematic representation of the atomic trajectories of each normal vibrational mode of naphthalene between 35 and 120 meV as determined by an ab initio calculation. The relative magnitudes of the arrows correspond to the atomic displacement in one-quarter of the overall vibration. Energies are provided in units of meV.

thalene, which were assigned to specific vibrations determined with ab initio methods (Figure 12), are apparent in the spectra of both inclusion compounds. The naphthalene-as-guest features, however, are better resolved in the brick structure owing to smaller contributions from the host lattice. Overall, the data suggest negligible influence of the host architecture, i.e., bilayer vs simple brick, on the dynamic behavior of the naphthalene guests.

Conclusions

The results described above further illustrate the capabilities of inelastic neutron scattering for probing molecular vibrations in organic solid-state compounds. The ability to selectivity deuterate the individual components—guanidinium ion, organodisulfonate pillar, and guest—of the ternary **GS** inclusion compounds significantly facilitates assignment of spectral features to each component. These assignments are further supported by ab initio calculations for individual guest molecules, which provides characterization of actual guest motions. Interestingly, calculated energies and amplitudes for these modes accurately reproduce the experimentally observed features for the guests confined within the host lattices and in crystals of the pure guests. This argues that the influence of the host on the dynamic behavior of the guest molecules is negligible, a characteristic that can be attributed to the absence of strong host−guest interactions in these crystals over the measured energy range. The results also suggest that the guest vibrations are not affected significantly by the host architecture surrounding the guest, as illustrated here for naphthalene guests in the bilayer and simple brick frameworks. Although it is likely that the vibrational behavior of the guest molecules included in the host framework departs significantly from that of the pure guests over the 0−35 meV range, spectra obtained from measurements conducted at these frequencies were unable to resolve any discernible peaks as a result of large phonon dispersion and provided no evidence to confirm this possibility. The vibrational behavior of the guanidinium ions, however, is sensitive to its supramolecular connectivity, as evidenced from differences in the INS features for bilayer and simple brick architectures with shifted ribbon and quasihexagonal hydrogen bonding motifs, respectively.

The work described herein also has demonstrated that INS spectra can be constructed through additive combination of spectra from ternary compounds prepared with isotopically substituted components. Also, INS spectra of a given host can be additively combined with the calculated spectrum of a guest to generate an INS spectrum that is essentially identical to that of the inclusion compound, as illustrated here for $\mathbf{G}_2$(**BPDS**)·3(anthracene). This demonstrates that INS spectra can be generated for a collection of inclusion compounds, based on the experimentally determined INS spectrum for a particular host and the calculated spectra for a variety of guest molecules, without actually collecting experimental data for each inclusion compound. More important, the self-consistency of the assignments based on different isotopically labeled combinations and the Gaussian 98 calculations demonstrates the reliability of ab initio calculations for characterizing guest vibrational modes and their energies.

Acknowledgment. The authors acknowledge the NIST Center for Neutron Research for allowing access to their experimental facilities. This work was supported by the MRSEC program of the National Science Foundation under Award Number DMR-9809364.

References and Notes

(1) Russell, V. A.; Etter, M. C.; Ward, M. D. *J. Am. Chem. Soc.* **1994**, *116*, 1941.

(2) Holman, K. T.; Ward, M. D. *Angew. Chem. Int. Ed.* **2000**, *39*, 1653. Swift, J. A.; Ward, M. D. *Chem. Mater.* **2000**, *12*, 1501. Holman, K. T.; Pivovar, A. M.; Swift, J. A.; Ward, M. D. *Acc. Chem. Res.* **2001**, *34*, 107. Swift, J. A.; Pivovar, A. M.; Reynolds, A. M.; Ward, M. D. *J. Am. Chem. Soc.* **1998**, *24*, 5887. Russell, V. A.; Evans, C.; Li, W.; Ward, M. D. *Science* **1997**, *276*, 575.

(3) Russell, V. A.; Evans, C. C.; Li, W.; Ward, M. D. *Science* **1997**, *276*, 575.

(4) Swift, J. A.; Pivovar, A. M.; Reynolds, A. M.; Ward, M. D. *J. Am. Chem. Soc.* **1998**, *120*, 5887.

(5) Holman, K. T; Martin, S. M.; Parker, D. P.; Ward, M. D. *J. Am. Chem. Soc.* **2001**, *123*, 4421.

(6) Pivovar, A. M.; Holman, K. T.; Ward, M. D. *Chem. Mater.* **2001**, *13*, 3018.

(7) (a) Carmona, P.; Molina, M.; Lasagabaster, A.; Escobar R.; Altabef, A. B. *J. Phys. Chem.* **1993**, *97*, 9519. (b) Middendorf, H. D.; Hayward, R.

L.; Parker, S. F.; Bradshaw J.; Miller, A. *Biophys. J.* **1995**, *69*, 660. (c) Nielsen O. F.; Oersted, H. C. *NATO ASI Ser., Ser. B* **1990**, *243*, 379. (d) Demmel, F.; Doster, W.; Petry W.; Schulte, A. *Eur. Biophys. J.* **1997**, *26*, 327. (e) Koloziejski, W.; Wawer, I.; Wozniak K.; Klinowski, J. *J. Phys. Chem.* **1993**, *97*, 12147. (f) Wolfs, I.; Desseyn, H. O. *Spectrochim. Acta, Part A* **1995**, *51A*, 1601.

(8) (a) Braden, D. A.; Hudson, B. S. *J. Phys. Chem. A* **2000**, *104*, 982. (b) Hudson, B. S. *J. Phys. Chem. A* **2001**, *105*, 3949. (c) Micu, A. M.; Durand, D.; Quilichini, M.; Field, M. J.; Smith, J. C. *J. Phys. Chem.* **1995**, *99*, 5645. (d) Loeffen, P. W.; Pettifer, R. F.; Fillaux, F.; Kearley, G. J. *J. Chem. Phys.* **1995**, *103*, 8444. (e) Tam, C. N.; Bour, P.; Eckert, J.; Trouw, F. R. *J. Phys. Chem. A* **1997**, *101*, 5877. (f) Bour, P.; Tam, C. N.; Sopkova, J.; Trouw, F. R. *J. Chem. Phys.* **1998**, *108*, 351. (g) Pawlukojc, A.; Natkaniec, I.; Grech, E.; Baran, J; Malarski, Z.; Sobczyk, L. *Spectrochim. Acta A* **1998**, *54*, 439. (h) Fernandez, M.; Navarro, A.; Lopez, J. J.; Tomkinson, J., Kearley, G. *Physica B* **1997**, *241*, 475. (i) Kemner, E.; de Schepper, I. M.; Kearley, G. J.; Jayasooriya, U. A. *J. Chem. Phys.* **2000**, *112*, 10926. (j) Yildirim, T.; Kilic, C.; Ciraci, S.; Gehring, P. M.; Neumann, D. A.; Eaton, P. E.; Emrick, T. *Chem. Phys. Lett.* **1999**, *309*, 234. (k) Bordallo, H. N.; Barthes, M.; Eckhart, J. *Physica B* **1998**, *241*−*243*, 1138. (l) Parker, S. F.; Braden, D. A.; Tomkinson, J.; Hudson, B. S. *J. Phys. Chem. B* **1998**, *102*, 5955. (m) Braden, D. A.; Parker, S. F.; Tomkinson, J.; Hudson, B. S. *J. Chem. Phys.* **1999**, *111*, 429. (n) Cser, L.; Holderna-Natkaniec, K.; Natkaniec, I.; Pawlukojc A. *Physica B* **2000**, *276*−*278*, 296. (o) Partal, F.; Fernandez-Gomez, M.; Lopez-Gonzalez, J. J.; Navarro, A.; Kearley, G. J. *Chem. Phys.* **2000**, *261*, 239. (p) Fernandez-Liencres, M. P.; Navarro, A.; Lopez-Gonzalez, J. J.; Fernandez-Gomez, M.; Tomkinson, J.; Kearley, G. J. *Chem. Phys.* **2001**, *266*, 1.

(9) Guillaume, F.; Sourisseau, C.; Dianoux, A. J. *J. Chem. Phys.* **1990**, *93*, 3536.

(10) Souaille, M.; Smith, J. C.; Guillaume, F. *J. Phys. Chem. B* **1997**, *101*, 6753.

(11) Girard, P.; Aliev, A. E.; Guillaume, F.; Harris, K. D. M.; Hollingsworth, M. D.; Dianoux, A. J.; Jonsen, P. *J. Chem. Phys.* **1998**, *10*, 4078.

(12) Paci, B.; Deleuze, M. S.; Caciuffo, R.; Tomkinson, J.; Ugozzoli, F.; Zerbetto, F. *J. Phys. Chem. A* **1998**, *102*, 6910.

(13) Paci, B.; Deleuze, M. S.; Caciuffo, R.; Arduini, A.; Zerbetto, F. *Mol. Phys.* **2000**, *9*, 567.

(14) Caciuffo, R.; Esposti, A. D.; Deleuze, M. S.; Leigh, D. A.; Murphy, A.; Paci, B.; Parker, S. F.; Zerbetto, F. *J. Chem. Phys.* **1998**, *109*, 11094.

(15) Leigh, D. A.; Parker, S. F.; Timpel, D.; Zerbetto, F. *J. Chem. Phys.* **2001**, *114*, 5006.

(16) Feldmann, J. *Helv. Chim. Acta* **1931**, *14*, 751.

(17) Trade names are mentioned in order to provide complete identification of experimental conditions and such identification is not intended as an endorsement by the NIST.

(18) Detailed information on the BT-4 FANS instrument can be found on the NCNR website at http://rrdjazz.nist.gov.

(19) Detailed information regarding *Gaussian 98* can be found at http://www.Gaussian.com.

(20) Trotter, J. *Acta Crystallogr.* **1961**, *14*, 1135.

(21) Szafranski, M. *Phys. Status Solidi B* **1997**, *201*, 343.

(22) Pivovar, A. M.; Yildirim, T.; Neumann, D. A.; Ward, M. D. *J. Chem. Phys.* **2001**, *115*, 1909.

(23) Takeuchi, H.; Suzuki, S.; Dianoux, A. J.; Allen, G. *Chem. Phys.* **1981**, *55*, 153.

(24) Natkaniec, I.; Nartowski, M.; Kulczycki, A.; Mayer, J.; Sudnik-Hrynkiewicz, M. *J. Mol. Struct.* **1978**, *46*, 503.

(25) Brock, C. P.; Dunitz, J. D. *Acta Cryst., Sect. B* **1990**, *46*, 795.

(26) Bokhenkov, E. L.; Kolesnikov, A. I.; Krivenko, T. A.; Sheka, E. F.; Demetjev, V. A.; Natkaniec, I. *J. Physique (C6)* **1981**, *42*, 605.

(27) Herringbone packing is also observed in pure naphthalene: Brock, C. P.; Dunitz, J. D. *Acta Crystallogr., Sect. B* **1982**, *38*, 2218.